



the problem of footstep planning and motion generation. In [8] the footstep planning component was done with a human-in-the-loop, and then a motion trajectory was optimized over those footstep locations. The human operator is taken out of the loop in [9] and proofs for optimality and completeness are available, but this comes at the cost of requiring convex collision-free regions for the robot to pass through. Optimization can also be used to generate dynamically stable periodic walking gaits and controllers, such as methods proposed in [10], [11].

The fourth category is the only one where probabilistically complete whole body motion planning is available. For this category, a mode is defined by a set of contacts between the robot and the environment. These contacts determine the feasibility constraints for any configurations associated with that mode. Methods in this category are usually used to navigate extremely rough terrain or plan whole body manipulation. As an example, Multi-modal PRM [12], Random-MMP [13], and related methods [14], [15] first sample modes in the environment and then generate whole body motions to transition through and between those modes. A configuration that transitions between two modes must satisfy the feasibility constraints of both modes simultaneously. Random-MMP is theoretically capable of navigating the semi-unstructured environments of this paper, but it struggles to find narrow passages, which may be important for navigating through challenging environments.

In this paper, we present the “Possibility Graph” for efficient whole body motion planning in semi-unstructured environments. By exploring the *possibility* of actions within a continuous search space, we can rapidly expand the search without being bottlenecked by expensive motion planning queries. We find that the Possibility Graph is effective at identifying passages which would be considered narrow by Random-MMP. We show that information from the Possibility Graph can be used to guide Random-MMP through narrow passages by focusing its sampling behavior. Together, these algorithms are able to traverse semi-unstructured environments on the order of seconds to minutes, depending on the complexity of the environment.

## II. PROBLEM SPECIFICATION

We seek to find feasible motion plans for a bipedal robot to traverse a “semi-unstructured” environment. In the context of this paper, we define “semi-unstructured” to mean that the terrain is structured—flat and even—but there are arbitrary unstructured obstacles throughout the environment. The robot may need to step over, duck under, or maneuver around these obstacles using whole body motions. The planner is provided with a kinematic model of the robot, a geometric model of all obstacles—including walls—and a layout of the floor. No other contextual information is provided to the planner (such as explicitly labelling doorways or passages).

## III. POSSIBILITY GRAPH

Motion planning methods ordinarily operate by constructing graphs or trees which consist of configurations that

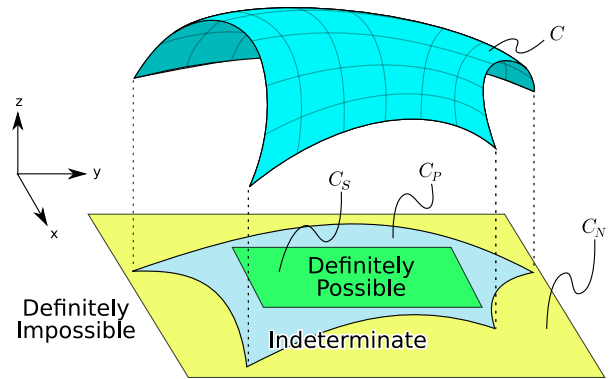


Fig. 2: Visual depiction of an abstract constraint manifold,  $C$  and its projection. The manifold is projected,  $C_P$ , from 3D space onto a plane. “Sufficient”  $C_S$  and “Necessary”  $C_N$  boundaries are fitted within and around the projection of the manifold. Elements inside the green box are definitely “Possible”. Elements outside of the yellow box are definitely “Impossible”. Elements inside the yellow box but outside of the green box are “Indeterminate” because they might or might not lie on the projection.

fully exist within the feasibility constraint manifold of the action they are performing. Remaining within this manifold is a reasonable requirement to place on the graph, because any vertices or edges which step outside of the manifold are, by definition, invalid—which may mean it is physically impossible, or simply harmful to the robot or its surroundings. Unfortunately, for a humanoid robot to remain on the constraint manifold, expensive calls to a whole body inverse kinematics (IK) solver must be performed [16]–[18]. This results in a critical bottleneck if a broad area needs to be explored before finding a solution.

The key idea of this work is to explore the *possibility* of an action first, instead of immediately committing to costly whole body inverse kinematics queries. The governing logical principles behind the Possibility Graph have a theoretical grounding in Possibility Theory [19], but the concepts are intuitive enough that a knowledge of Possibility Theory is not necessary to proceed. It is enough to understand that the *possibility* of any given action  $e$  can be labelled with “impossible”, “possible”, or “indeterminate” depending on whether it satisfies the necessary condition ( $C_N$ ) or the sufficient condition ( $C_S$ ) that are assigned to it:

$$e.\text{label} = \begin{cases} \text{“impossible”} & \text{if } C_N(e) \text{ is false} \\ \text{“possible”} & \text{if } C_S(e) \text{ is true} \\ \text{“indeterminate”} & \text{otherwise} \end{cases} \quad (1)$$

If we design necessary and sufficient conditions that can be checked much more quickly than querying the original constraint manifold, we can then construct a *Possibility Graph*, whose states (vertices) are connected by either “possible” or “indeterminate” actions (edges), and expand it very efficiently for whole body motion planning.

### A. Simplifying the Manifold: Sufficient vs. Necessary

To construct the Possibility Graph, we must first design sufficient and necessary conditions for the feasibility con-

straint manifold of the action whose possibilities we are exploring. We should design the conditions to be quick to test in order to reduce the computation of exploration. The conditions should also use as few parameters as is reasonable, because randomized search methods tend to be more effective in low-dimensional search spaces.

Suppose we have a 2D constraint manifold,  $C$ , which exists in 3D space (Fig. 2). Let the  $xy$ -plane be a low-dimensional feature space which contains the essential information for navigating  $C$ . We denote the projection of  $C$  by  $C_p$ . Even with a flattened-out projection, identifying which points are inside or outside of the manifold may still be costly or difficult, because the boundary of  $C_p$  may consist of functions that are expensive to compute or hard to fully define. However, suppose a box, circle, or some other simple shape can be fit within  $C_p$  such that it is *guaranteed* that every point within the simple shape also lies within the manifold projection. Such a shape would be a suitable representation of the sufficient condition manifold,  $C_S$ . Any point lying inside of  $C_S$  also lies inside of  $C_p$  and should be labelled with “possible”. Similarly, if  $C_p$  can be bounded by a simple shape,  $C_N$ , such that  $C_p \subseteq C_N$ , then  $C_N$  would qualify as the necessary condition manifold. Any point lying outside of  $C_N$  should be labelled with “impossible”. Finally, any point inside of  $C_N$  but outside of  $C_S$  should be labelled with “indeterminate”.

### B. Possibility Graph Construction

*Definition 1:* A Possibility Graph is a tuple

$$PG = (\mathcal{E}, \Gamma_{PG} = (V, E), Q_{Confirmation}) \quad (2)$$

where,

- $\mathcal{E}$  is the “exploration space” for the graph,
- $\Gamma_{PG}$  is a graph consisting of vertices  $V$  and edges  $E$ ,
- $V$  is a set of vertices which are elements of  $\mathcal{E}$ ,
- $E$  is a set of directed edges that transition between vertices using actions,
- $Q_{Confirmation}$  is a queue which manages confirmation jobs.

The input to our path finding algorithm (Algorithm 1) is a “start” vertex and one or more “goals” vertices in  $\mathcal{E}$ . Each of these input vertices will serve as the root vertex of a subgraph. At each iteration, we attempt to expand the subgraphs towards a randomly selected point in  $\mathcal{E}$  and connect the subgraphs to vertices that already exist in other disjoint subgraphs. The algorithm terminates when a valid path from “start” to any of the “goals” is found or when the computational time budget is exceeded.

Algorithm 2 describes how the graph is being expanded at each iteration. It works similarly to CBIIRRT, but with some small modifications. For each subgraph, we find the vertex which is closest to the sampled point,  $p_{target} \in \mathcal{E}$ . The list of these vertices is sorted according to which one is closest to the  $p_{target}$ . We expand from the closest vertex towards the target until the necessary conditions are no longer satisfied. The second closest subgraph is expanded towards the last vertex that was generated in the previous step, in an attempt

---

### Algorithm 1: Finding a path by exploring possibilities

---

```

1 Function FindPath(start, goals)
2    $\Gamma_{PG}.V \leftarrow \{\text{start}, \text{goals}\};$ 
3    $Q_{Confirmation}.launchThreads();$ 
4    $t \leftarrow 0;$ 
5   while  $t < t_{max}$  do
6      $p_{target} \leftarrow \text{RandomSample}();$ 
7      $\{\Gamma_{PG}.V, \Gamma_{PG}.E\}.append(\text{Expand}(p_{target}));$ 
8     for  $v$  in goals do
9       if  $\text{Connected}(\text{start}, v)$  then
10         $\Gamma_{path} \leftarrow \text{ShortestPath}(\text{start}, v);$ 
11        if  $\text{ConfirmPath}(\Gamma_{PG}, \Gamma_{path},$ 
12           $Q_{Confirmation})$  then
13          return  $\Gamma_{path};$ 
14         $t \leftarrow \text{CurrentTime}();$ 
15 return null;

```

---

to connect the subgraphs together and merge them into one. However, in the case when both the first and second closest subgraphs are already connected to the goal vertices, merging together these two subgraphs is not productive for finding a solution. As such, we select another subgraph by finding the next closest vertex whose subgraph is not currently connected to a goal vertex.

The details of connecting two vertices,  $v_{start}$  and  $p_{target}$  are described in Algorithm 3. Starting from  $v_{start}$ , the Connect routine incrementally adds vertices to the subgraph of  $v_{start}$  toward  $p_{target}$ . For a vertex to be added to the subgraph, the edge (action) connecting to it must at least satisfy  $C_N$ . If the edge also satisfies  $C_S$ , it is labelled with “possible”. Otherwise, it is labelled with “indeterminate”.

---

### Algorithm 2: Growing the graph

---

```

1 Function Expand( $p_{target}$ )
2    $Q_{closest} \leftarrow \text{new SortedVertexQueue};$ 
3   for  $g$  in  $\Gamma_{PG}.SubGraphs$  do
4      $v \leftarrow g.\text{FindClosestVertexTo}(p_{target});$ 
5      $Q_{closest}.insert(\text{dist}(v, p_{target}), v);$ 
6    $v_0 \leftarrow Q_{closest}.pop\_front();$ 
7    $\{V_{new}, E_{new}\} \leftarrow \text{Connect}(v_0, p_{target});$ 
8    $p_{target} \leftarrow V_{new}.back();$ 
9   if  $\text{UpstreamFromGoal}(v_0)$  then
10    while  $\text{UpstreamFromGoal}(Q_{closest}.front())$  do
11       $Q_{closest}.pop\_front();$ 
12    $v_1 \leftarrow Q_{closest}.pop\_front();$ 
13    $\{V_{new}, E_{new}\}.append(\text{Connect}(v_1, p_{target}));$ 
14   return  $\{V_{new}, E_{new}\};$ 

```

---

In addition, a projection step is performed when adding a vertex to the subgraph in the Connect routine. The probability of an edge that satisfies  $C_N$  or  $C_S$  may be low if the volumes of the condition manifolds within  $\mathcal{E}$  are thin. Condition manifolds of this nature must be provided with a projection operator, similar to CBIIRRT [20]. The projection operator must take an arbitrary point in  $\mathcal{E}$  and attempt to move it to the nearest point on the condition manifold.

---

**Algorithm 3:** Connecting the graph to a target

---

```
1 Function Connect( $v_{\text{start}}, p_{\text{target}}$ )
2    $\{V_{\text{new}}, E_{\text{new}}\} \leftarrow \{\text{new VertexQueue, new EdgeQueue}\};$ 
3    $v_{\text{last}} \leftarrow v_{\text{start}};$ 
4    $v \leftarrow \text{ExtendTowards}(v_{\text{start}}, p_{\text{target}});$ 
5    $v_p \leftarrow \text{Project}(v);$ 
6   while  $v \neq p_{\text{target}}$  do
7      $e \leftarrow \text{Edge}(v_{\text{last}}, v_p);$ 
8     if not  $C_N(e)$  then
9       break;
10     $e.\text{label} \leftarrow \text{indeterminate};$ 
11    if  $C_S(e)$  then
12       $e.\text{label} \leftarrow \text{possible};$ 
13     $\{V_{\text{new}}, E_{\text{new}}\}.\text{append}(\{v_p, e\});$ 
14     $v_{\text{last}} \leftarrow v_p;$ 
15     $v \leftarrow \text{ExtendTowards}(v, p_{\text{target}});$ 
16     $v_p \leftarrow \text{Project}(v);$ 
17  return  $\{V_{\text{new}}, E_{\text{new}}\};$ 
```

---

### C. Path Confirmation

Once a start-connected subgraph has merged with a goal-connected subgraph, a candidate for the solution path becomes available. However, if any edges along this path are *indeterminate*, then a deeper inspection is needed to determine whether the path is truly a feasible solution (Algorithm 4). These edges are passed into the “Confirmation Queue” as “Confirmation Jobs” while simultaneously being removed from the Possibility Graph. In parallel threads, the “Confirmation Jobs” are pulled out of the queue, and a low-level whole body motion planner (preferably one that is probabilistically complete) is queried to determine whether the edge is truly feasible. If every “indeterminate” edge along a candidate path is validated by the motion planner, the validity of the solution is confirmed. If any “indeterminate” edge in the path turns out invalid, the confirmation is negative.

In practice, we can further improve the performance by allowing the `ConfirmPath` routine to update the Possibility Graph, even when the path is not valid. When an edge is deemed infeasible, we can still return whatever portion of the path is feasible to the Possibility Graph, now with the “possible” label instead of “indeterminate”.

Since these jobs are performed in parallel threads, the Possibility Graph itself can continue to grow while the expensive low-level planners are running. This provides the Possibility Graph with the opportunity to seek out alternate solutions which are easier to compute, instead of being bottlenecked by prohibitively expensive planning queries which might not prove fruitful.

## IV. WALKING IN SEMI-UNSTRUCTURED ENVIRONMENTS

Planning a path through a semi-unstructured environment entails finding a physically feasible sequence of footsteps—combined with whole body motions that are constrained to those footsteps—which move the robot from the start configuration to the goal configuration. To apply the Possibility Graph to the problem of walking in semi-unstructured

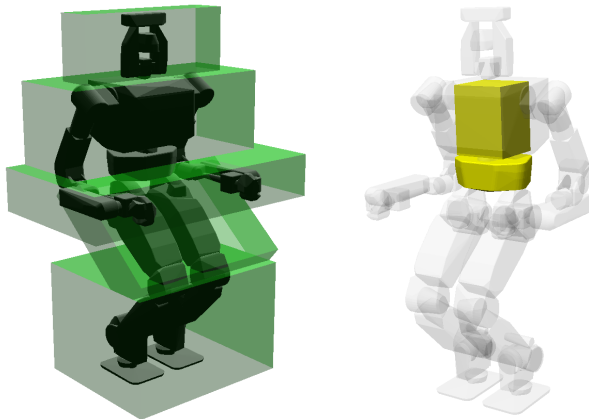
---

**Algorithm 4:** Confirm a path

---

```
1 Function ConfirmPath( $\Gamma_{PG}, \Gamma_{\text{path}}, Q_{\text{Confirmation}}$ )
2    $\text{pathConfirmed} \leftarrow \text{true};$ 
3   for  $e$  in  $\Gamma_{\text{path}}.E$  do
4      $\text{edgeConfirmed} \leftarrow \text{false};$ 
5     if  $e.\text{label} \equiv \text{possible}$  then
6        $\text{edgeConfirmed} \leftarrow \text{true};$ 
7     else if  $e.\text{label} \equiv \text{indeterminate}$  then
8        $\Gamma_{PG}.\text{remove}(e);$ 
9        $Q_{\text{Confirmation}}.\text{insert}(\text{SpawnConfirmationJob}(e));$ 
10    if  $\text{edgeConfirmed} \equiv \text{false}$  then
11       $\text{pathConfirmed} \leftarrow \text{false};$ 
12  return  $\text{pathConfirmed};$ 
```

---



(a) Bounding geometry used for sufficient conditions (Green)      (b) Minimal geometry used for necessary conditions (Yellow)

Fig. 3: Collision geometries used for the (a) sufficient and (b) necessary conditions. Since (a) occupies more space, the constraint manifold for the sufficient conditions is smaller—and therefore more restrictive—than the manifold for the necessary conditions.

environments, we must first define the feature space for route exploration, as well as the sufficient and the necessary conditions that pertain to the robot’s ability to take steps and move its whole body.

### A. Possibility Exploration Space

The vertices of the Possibility Graph exist in the possibility exploration space,  $\mathcal{E}$ . For the problem of walking in semi-unstructured environments, we define  $\mathcal{E}$  as  $SE(3)$ , which offers enough parameters to design effective sufficient and necessary conditions. Each point in  $\mathcal{E}$  represents a transformation of the robot’s root (pelvis) link. As we generate edges in  $\mathcal{E}$ , we are creating routes to guide the root link towards its destination. Figure 4 illustrates what a section of a Possibility Graph may look like.

### B. Sufficient Conditions

We define the sufficient conditions by first constructing a bounding box which encapsulates all the motions that the robot might exhibit while walking or turning in any direction

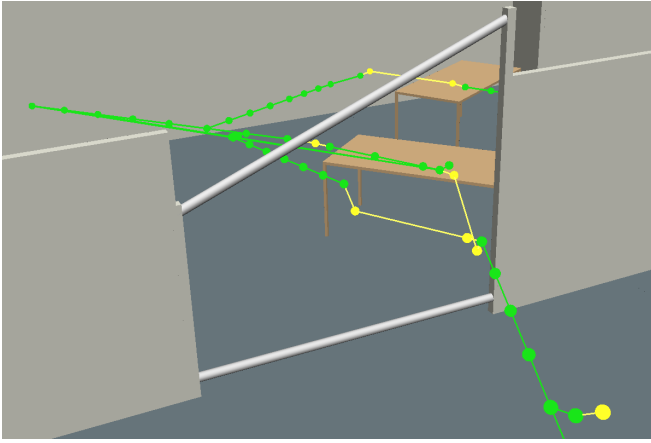


Fig. 4: Snapshot of a Possibility Graph. Green edges are “Possible”; yellow edges are “Indeterminate”. Portions of the graph that are in wide open hallways are Possible, whereas elements that squeeze between obstacles are Indeterminate.

using some basic gait generator. The bounding geometry can be seen in Fig. 3a. If nothing in the environment is colliding with this geometry, then the robot is guaranteed to not collide with anything while performing its normal gait. For this condition, validating an edge  $e(v_a, v_b)$  in SE(3) involves applying every SE(3) transformation (or a representatively dense sampling of them) from  $v_a$  to  $v_b$  to the bounding geometry and checking the collision with the environment. In addition, we require that the corners of the support polygon of each foot must be fully supported by solid ground while the robot stands in the nominal configuration shown in Fig. 3. The basic gait generator will guarantee that joint position and torque limits will be met, so long as the bounding geometry and support polygon conditions are met.

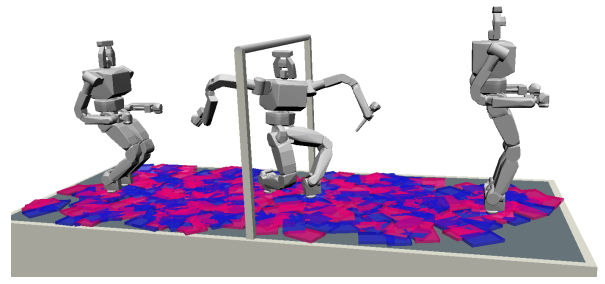
### C. Necessary Conditions

The necessary conditions are much less restrictive than the sufficient conditions. The collision geometry used for the necessary conditions can be seen in Fig. 3b. This minimal collision geometry is a subset of the actual robot’s collision geometry. This subset is chosen such that it is completely unaffected by any joint motion (assuming the root link remains fixed in place). Therefore, if this geometry is in collision with any obstacles, then the robot is guaranteed to be in collision, no matter what its joint positions are. If this minimal geometry cannot sweep along an edge, then that edge is considered “impossible” and is left out of the Possibility Graph.

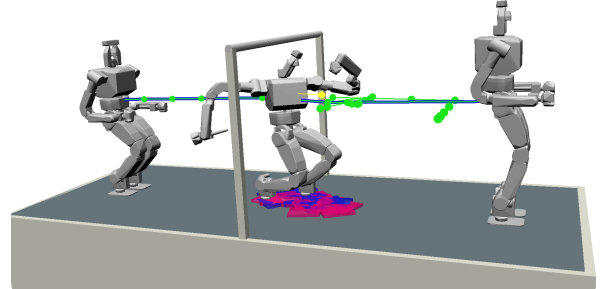
### D. Guided Multi-modal Planning

Once the sufficient and necessary conditions are defined, the only remaining decision in our algorithm is the choice of whole body motion planner. In this work, we use Random-MMP introduced by Hauser et. al. [13] as our low-level planner because it is able to solve general motion planning problems with frequent changes in contacts (i.e. modes).

Random-MMP by itself can solve the semi-unstructured problems posed in this paper with the theoretical property



(a) Uninformed Random-MMP: Exhaustive search



(b) Guided-MMP: Focuses the search around the indeterminate (yellow) edge of the Possibility Graph.

Fig. 5: Limbo scenario. The difference in search behaviors for uninformed (a) versus guided (b) versions of Random-MMP. Blue and magenta rectangles are the foot placements of the left and right (respectively) feet for each sampled mode.

of probabilistic completeness. However, Random-MMP performs best when it is able to utilize informed sampling. For example, when used for manipulation, Random-MMP should be provided with information on how to sample a state that is within the reachable region of the manipulatable target. In this paper, we aim to solve problems where extra contextual information is not provided, meaning Random-MMP on its own could take prohibitively long to find a solution.

A key advantage of the Possibility Graph is that indeterminate edges can be used to guide low-level planners. Therefore, even though the original problem does not provide us with information about passages in the environment, indeterminate edges can be considered potential passages that are worthy of further inspection. This allows us to turn an uninformed search into an informed search. We will refer to this as Guided-MMP to distinguish it from uninformed Random-MMP. Figure 5 illustrates the difference in behavior between these methods. The uninformed search takes tens of minutes whereas the guided search takes tens of seconds. The only difference between the uninformed vs. guided approaches is that the guided approach focuses its randomized mode and configuration samples to be near the indeterminate edges, according to a Normal Distribution. Meanwhile, the uninformed search has no choice but to broadly sample the entire domain.

## V. EXPERIMENTS

We present two virtual experimental scenarios. The first scenario, shown in Fig. 5, is referred to as the “Limbo Scenario”. The robot must traverse from one side of the

TABLE I: Time performance results tested on an Intel<sup>®</sup> Xeon<sup>®</sup> Processor E3-1290 v2 (8M Cache, 3.70 GHz) with 16GB of RAM. This table shows the time spent (in seconds) and the rate of success for 30 trials of each scenario and each variation. The standard deviation is given in parentheses. Numerous trials are run because randomized planners have non-deterministic run times and non-deterministic success rates. All trials were given a one-hour timeout, at which point we consider the trial to have failed.

Scenario	Uninformed Random-MMP		Possibility Graph	
	Time	Success	Time	Success
Limbo Scenario (Fig. 5)	2355.5 (1000.3)	86.67%	20.56 (26.51)	100%
Four Routes Scenario (Fig. 6)	3600 (0)	0%	68.44 (33.98)	96.67%
West Door Blocked (Fig. 7b)	3600 (0)	0%	295.54 (205.847)	96.67%
East Door Blocked (Fig. 7c)	3600 (0)	0%	349.60 (195.38)	100%
Bars Removed (Fig. 7d)	3600 (0)	0%	7.31 (5.73)	100%

platform to the other while ducking underneath a limbo bar. It demonstrates the performance difference between an uninformed Random-MMP search versus Guided-MMP which is supplemented by the Possibility Graph. Even in such a simple scenario, the Possibility Graph improves performance by two orders of magnitude.

The second scenario is referred to as the “Four Routes Scenario”. It demonstrates some of the larger scale capabilities of the Possibility Graph. The robot must navigate from the southwest corner to the northeast corner of the floor. Each room has two entrances, making a total of four possible routes the robot may choose from. Each doorway has its own challenges associated with passing through it, seen in Fig. 1.

The route which is easiest for the planner to find passes through the west doorway, down the hallway, and then through the east doorway as shown in Fig 7a. Those doorways are the easiest to plan for because they have the most “expansiveness” as defined in [21]. Since the planner chooses the first successful plan that it finds, this will be the most commonly chosen route (although the randomized nature of the planner does not guarantee that this will always be the chosen route). We can tweak the environment to force the robot to find a path through the south doorway by blocking off the west doorway (as in Fig. 7b). Similarly, the robot can be forced to find a path through the north doorway by blocking off the east (as in Fig. 7c). Each of these modifications result in considerably longer run times as shown in Table I. This shows that when the planner is not required to find routes through challenging regions, it will naturally tend to favor expansive regions where it can find paths easily.

In some cases, there may be a clear path from the start to the goal. To simulate this, in Fig. 7d we remove the bars that are obstructing the north and south doorways. The result is a much leaner graph and very short plan time as seen in Table I.

## VI. CONCLUSIONS

This work presented a new high-level algorithm for identifying routes in semi-unstructured environments, and a way to leverage this information in lower-level motion planners. The method presented improves performance of existing algorithms by orders of magnitude, making difficult large-scale problems tractable when they would not have been previously.

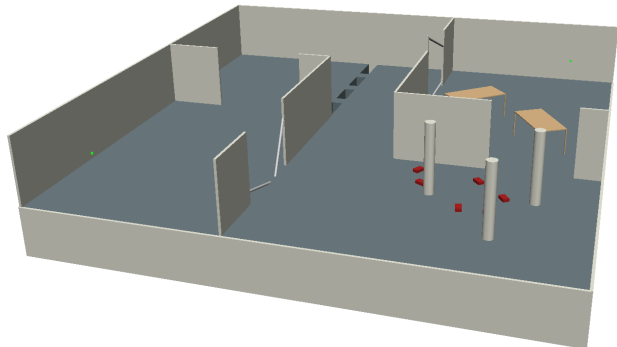
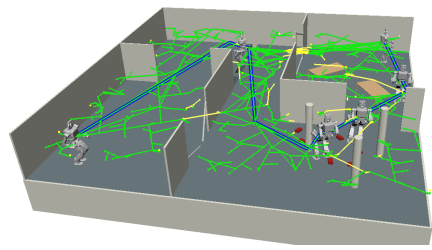


Fig. 6: Basic “Four Routes” scenario.

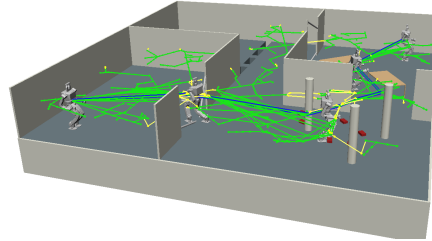
The motivation of the Possibility Graph is similar to a Fuzzy PRM [22]: Improve search performance by making broad exploration less expensive and focusing heavy computations on paths that are likely to achieve a goal. However, the Possibility Graph is grounded in Possibility Theory which allows us to make definitive statements about action possibilities using low-dimensional condition manifolds. This is in contrast to Fuzzy PRM which estimates the probability of an action being feasible using statistical methods. Fuzzy PRM does not make any changes to the dimensionality of the problem or the computational cost of testing the feasibility constraints; it simply concentrates the feasibility tests along paths that it estimates as being likely to lead to the goal.

Future work will investigate other ways that the Possibility Graph can be leveraged to generate plans. For example, the graph could consider the possibilities of actions besides walking, or dynamic actions rather than quasi-static actions. It would also be natural to use a variety of low-level planners that could compete to confirm indeterminate edges rather than using a catch-all probabilistically complete low-level planner which might not perform particularly well in all scenarios.

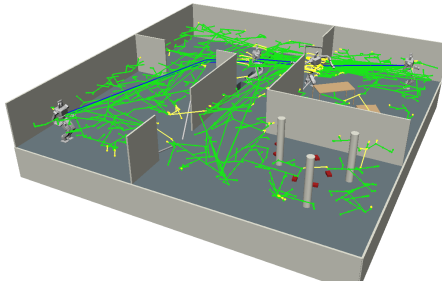
The completeness of the Possibility Graph is currently an open question. Future work will examine under what conditions the Possibility Graph may be considered probabilistically complete. This will likely depend on the completeness of the low-level planners available to the Possibility Graph.



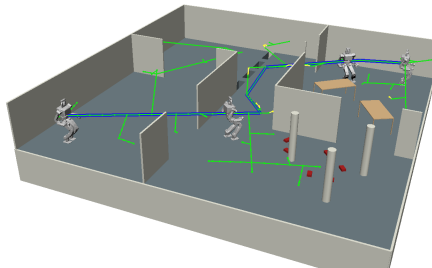
(a) Solution for the standard variation of the scenario



(b) Solution when the west doorway is blocked off



(c) Solution when the east doorway is blocked off



(d) Solution with bars removed from the north and south

Fig. 7: Variations of the “Four Routes Scenario”.

#### ACKNOWLEDGMENTS

This work was supported by DARPA grant D15AP00006.

#### REFERENCES

- [1] J. Pettré, J.-P. Laumond, and T. Siméon, “A 2-stages locomotion planner for digital actors,” in *Proceedings of the 2003 ACM SIGGRAPH/Eurographics symposium on Computer animation*. Eurographics Association, 2003, pp. 258–264.
- [2] N. Perrin, O. Stasse, F. Lamiroux, Y. J. Kim, and D. Manocha, “Real-time footstep planning for humanoid robots among 3d obstacles using a hybrid bounding box,” in *Robotics and Automation (ICRA), 2012 IEEE International Conference on*. IEEE, 2012, pp. 977–982.

- [3] J. J. Kuffner, K. Nishiwaki, S. Kagami, M. Inaba, and H. Inoue, “Footstep planning among obstacles for biped robots,” in *Intelligent Robots and Systems, 2001. Proceedings. 2001 IEEE/RSJ International Conference on*, vol. 1. IEEE, 2001, pp. 500–505.
- [4] J. Kuffner, S. Kagami, K. Nishiwaki, M. Inaba, and H. Inoue, “Online footstep planning for humanoid robots,” in *Robotics and Automation, 2003. Proceedings. ICRA’03. IEEE International Conference on*, vol. 1. IEEE, 2003, pp. 932–937.
- [5] J. Chestnutt, J. Kuffner, K. Nishiwaki, and S. Kagami, “Planning biped navigation strategies in complex environments,” in *IEEE Int. Conf. Hum. Rob., Munich, Germany, 2003*.
- [6] J. Garimort, A. Hornung, and M. Bennewitz, “Humanoid navigation with dynamic footstep plans,” in *Robotics and Automation (ICRA), 2011 IEEE International Conference on*. IEEE, 2011, pp. 3982–3987.
- [7] N. Perrin, O. Stasse, L. Baudouin, F. Lamiroux, and E. Yoshida, “Fast humanoid robot collision-free footstep planning using swept volume approximations,” *IEEE Transactions on Robotics*, vol. 28, no. 2, pp. 427–439, 2012.
- [8] M. Fallon, S. Kuindersma, S. Karumanchi, M. Antone, T. Schneider, H. Dai, C. P. D’Arpino, R. Deits, M. DiCicco, D. Fourie, et al., “An architecture for online affordance-based perception and whole-body planning,” *Journal of Field Robotics*, vol. 32, no. 2, pp. 229–254, 2015.
- [9] R. Deits and R. Tedrake, “Footstep planning on uneven terrain with mixed-integer convex optimization,” in *2014 IEEE-RAS International Conference on Humanoid Robots*. IEEE, 2014, pp. 279–286.
- [10] A. Hereid, E. A. Cousineau, C. M. Hubicki, and A. D. Ames, “3d dynamic walking with underactuated humanoid robots: A direct collocation framework for optimizing hybrid zero dynamics,” in *IEEE International Conference on Robotics and Automation (ICRA). IEEE, 2016*.
- [11] M. J. Powell, H. Zhao, and A. D. Ames, “Motion primitives for human-inspired bipedal robotic locomotion: walking and stair climbing,” in *Robotics and Automation (ICRA), 2012 IEEE International Conference on*. IEEE, 2012, pp. 543–549.
- [12] K. Hauser and J.-C. Latombe, “Multi-modal motion planning in non-expansive spaces,” *The International Journal of Robotics Research*, 2009.
- [13] K. Hauser and V. Ng-Thow-Hing, “Randomized multi-modal motion planning for a humanoid robot manipulation task,” *The International Journal of Robotics Research*, vol. 30, no. 6, pp. 678–698, 2011.
- [14] K. Hauser, T. Bretl, J.-C. Latombe, K. Harada, and B. Wilcox, “Motion planning for legged robots on varied terrain,” *The International Journal of Robotics Research*, vol. 27, no. 11–12, pp. 1325–1349, 2008.
- [15] T. Bretl, S. Lall, J.-C. Latombe, and S. Rock, “Multi-step motion planning for free-climbing robots,” in *Algorithmic Foundations of Robotics VI*. Springer, 2004, pp. 59–74.
- [16] L. Sentis and O. Khatib, “A whole-body control framework for humanoids operating in human environments,” in *Proceedings 2006 IEEE International Conference on Robotics and Automation, 2006. ICRA 2006*. IEEE, 2006, pp. 2641–2648.
- [17] T. Sugihara and Y. Nakamura, “Whole-body cooperative balancing of humanoid robot using cog jacobian,” in *Intelligent Robots and Systems, 2002. IEEE/RSJ International Conference on*, vol. 3. IEEE, 2002, pp. 2575–2580.
- [18] M. Gienger, H. Janssen, and C. Goerick, “Task-oriented whole body motion for humanoid robots,” in *5th IEEE-RAS International Conference on Humanoid Robots, 2005*. IEEE, 2005, pp. 238–244.
- [19] D. Dubois and H. Prade, *Possibility theory: an approach to computerized processing of uncertainty*. Springer Science & Business Media, 2012.
- [20] D. Berenson, S. Srinivasa, D. Ferguson, and J. Kuffner, “Manipulation planning on constraint manifolds,” in *IEEE International Conference on Robotics and Automation (ICRA ’09)*, May 2009, pp. 625–632.
- [21] D. Hsu, J.-C. Latombe, and R. Motwani, “Path planning in expansive configuration spaces,” in *Robotics and Automation, 1997. Proceedings., 1997 IEEE International Conference on*, vol. 3. IEEE, 1997, pp. 2719–2726.
- [22] C. L. Nielsen and L. E. Kavraki, “A two level fuzzy prm for manipulation planning,” in *Intelligent Robots and Systems, 2000. (IROS 2000). Proceedings. 2000 IEEE/RSJ International Conference on*, vol. 3. IEEE, 2000, pp. 1716–1721.